

RESEARCH

Open Access



Predictive modeling of graves' orbitopathy activity based on meibomian glands analysis using in vivo confocal microscopy

Zixuan Su^{1†}, Yayan You^{2†}, Shengnan Cheng^{3†}, Jiahui Huang¹, Xueqing Liang⁴, Xinghua Wang^{1*} and Fagang Jiang^{1*}

Abstract

Objectives This study aims to identify indicators of disease activity in patients with graves' orbitopathy (GO) by examining the microstructural characteristics of meibomian glands (MGs) and developed a diagnostic model.

Methods We employed in vivo confocal microscopy (IVCM) to examine MGs in GO patients. Patients classified in the active phase were determined based on the clinical activity score (CAS). The research employed the least absolute shrinkage and selection operator (LASSO) method to select key indicators. Subsequently, a logistic regression model was constructed to predict GO disease activity.

Results A total of 45 GO patients, corresponding to 90 eyes, were included in this study. A Lasso regression algorithm was utilized to select the predictor variables. Five predictor variables were included in our diagnostic model ultimately. The area under the curve (AUC) for the training set model reached 0.959, and for the validation set was 0.969. The training set and validation set models both demonstrated high accuracy in calibration. Finally, a Nomogram chart was constructed to visualize the diagnostic model.

Conclusion We constructed a diagnostic model based on microstructural indicators of MGs obtained through IVCM and offered a clinical utility for assessing GO disease activity, aiding in the diagnosis and selection of treatment strategies for GO.

Key message

What is known?

- Several studies have demonstrated an association between Graves' Orbitopathy (GO) severity and increased ocular surface exposure. In vivo confocal microscopy revealed distinct microstructural characteristics of Meibomian Glands (MGs) in GO patients compared to healthy individuals.

[†]Zixuan Su, Yayan You and Shengnan Cheng were contributed equally to the manuscript as joint first authors.

*Correspondence:

Xinghua Wang
xinghua_wang@hust.edu.cn
Fagang Jiang
fjjiang@hust.edu.cn

Full list of author information is available at the end of the article



© The Author(s) 2025. **Open Access** This article is licensed under a Creative Commons Attribution-NonCommercial-NoDerivatives 4.0 International License, which permits any non-commercial use, sharing, distribution and reproduction in any medium or format, as long as you give appropriate credit to the original author(s) and the source, provide a link to the Creative Commons licence, and indicate if you modified the licensed material. You do not have permission under this licence to share adapted material derived from this article or parts of it. The images or other third party material in this article are included in the article's Creative Commons licence, unless indicated otherwise in a credit line to the material. If material is not included in the article's Creative Commons licence and your intended use is not permitted by statutory regulation or exceeds the permitted use, you will need to obtain permission directly from the copyright holder. To view a copy of this licence, visit <http://creativecommons.org/licenses/by-nc-nd/4.0/>.

- The Clinical Activity Score (CAS) serves as a widely adopted tool for evaluating GO activity. However, its precision is compromised by inter-assessor variability, particularly when non-ophthalmologists are involved in the assessment.

What is new?

- This study introduces a novel diagnostic model for evaluating GO activity by utilizing In Vivo Confocal Microscopy (IVCM) to quantify changes in the microstructure of MGs.
- The predictive model achieved strong performance with an Area Under the Curve (AUC) of 0.959 for the training set and 0.969 for the validation set, underscoring its reliability, repeatability, and generalizability, establishing it as a valuable tool to aid in the diagnosis of GO.

Keywords Graves' orbitopathy, Meibomian glands, In vivo confocal microscopy, Clinical activity score, Diagnostic model.

Introduction

Graves' orbitopathy (GO) is an autoimmune inflammatory disease that can trigger inflammation in and around the eye, having the highest incidence rate among adult orbital diseases [1–3]. Commonly, GO patients present with conjunctival hyperemia and edema, dry eye, superficial keratitis, and exposure keratopathy, among which dry eye is the most frequent cause of ocular discomfort in GO patients [4, 5]. Some studies have found that the prevalence of dry eye disease in active GO is higher than in the inactive phase, and the severity of ocular surface exposure may increase with the severity of GO [6–8].

The European Group on Graves' Orbitopathy (EUGOGO) has reported a classification of GO based on its severity into mild, moderate-to-severe, and very severe stages [9]. The Clinical Activity Score (CAS) used for evaluating GO activity [10]. The evaluation of GO activity serves as a crucial guide for formulating treatment plans, determining the optimal timing for surgery, and conducting prognostic assessments. This evaluation plays a pivotal role in guiding treatment strategies, determining the optimal timing for surgical interventions, and conducting prognostic assessments. Notably, initiating treatment within the first year of disease has demonstrated superior treatment outcomes for GO patients [9]. The CAS is characterized by its simplicity, clarity, and operational efficiency. Its user-friendly nature enhances its potential for widespread application. However, it is essential to acknowledge that the CAS can be influenced by subjective factors from both examiners and patients. Consequently, clinical practice integrating the CAS with findings from orbital magnetic resonance imaging (MRI) examinations for staging purposes. Recognizing the limitations associated with MRI in terms of patient acceptance and feasibility in daily clinical practice, there is an urgent need for innovative auxiliary diagnostic methods.

In vivo confocal microscopy (IVCM) is a potent tool that enables high-resolution observation of various ocular surface structures at the cellular level [11, 12]. It can be used to assess the live cells of the cornea [13], conjunctiva [14, 15], and meibomian gland [16, 17] in GO

patients, primarily employed to evaluate the features of conjunctival tissue, corneal tissue, and sub-basal nerve plexus [5, 13]. Recent IVCM studies by Vagge et al. on the microscopic structural changes in GO patients' meibomian glands (MGs) found a decrease in MGs acinar density and an increase in ductal area, longest and shortest diameter of acini. They also discovered that the MGs ductal area was negatively correlated with Schirmer's test (SIT), while acinar density was positively correlated with tear break-up time (TBUT) [17]. Furthermore, Wei et al., through in vivo confocal microscopy, detected a reduced goblet cell density (GCD) in GO patients compared to a healthy control group [14]. In our previous studies, we also identified substantial differences in the microscopic structure of MGs between GO patients and the control group. Moreover, a notable correlation was observed between the microscopic structure of MGs and CAS [16].

Consequently, it is crucial to investigate novel and effective approaches for assessing the activity of GO to enhance the precision of staging and management of GO patients in conjunction with the CAS. The primary objective of this study is to develop a diagnostic model for evaluating GO activity by utilizing MGs microscopic indicators detected via IVCM. This innovative approach aims to refine the accuracy of GO patient staging, thereby facilitating more precise clinical interventions.

Methods

Ethical approval

This study in compliance with ethical standards and institutional regulations, this research was conducted following the approval obtained from the Institutional Review Board of Union Hospital, Tongji Medical College, Huazhong University of Science and Technology, approval number 20,220,293. The research adhered to all ethical guidelines, ensuring the rights, safety, and confidentiality of the participants. Informed consent was obtained from all participants, and their privacy was carefully protected throughout the study, following the principles outlined in the Declaration of Helsinki.

Patient selection

This prospective study incorporated a cohort of 45 patients (90 eyes) with GO who sought outpatient or inpatient care at Union Hospital, Tongji Medical College, Huazhong University of Science and Technology from May 2022 to January 2023. The diagnosis was established based on the Bartley criteria [18], which require the presence of eyelid retraction, in conjunction with at least one of the following: thyroid dysfunction, proptosis, extraocular muscle involvement, or visual nerve impairment. In cases where there is no eyelid retraction, thyroid dysfunction, in addition to one of the aforementioned criteria, is necessary for diagnosis.

Patients were stratified using the CAS to assess seven distinct parameters, including spontaneous retrobulbar pain, pain on eye movement, eyelid edema, eyelid erythema, conjunctival edema, conjunctival erythema, and caruncle swelling. Each parameter was assigned a score of 1, with a CAS score of ≥ 3 indicating the active phase, and a CAS score of < 3 signifying the inactive phase [9].

Inclusion and exclusion criteria

Patients were considered eligible for the study if they fulfilled the following criteria: (1) Participants aged over 18, with no gender restrictions; (2) The case group comprised individuals diagnosed with GO; (3) All study subjects participated voluntarily. The exclusion criteria were: (1) Use of ocular medications such as anti-inflammatory agents and artificial tears in the past three months; (2) A history of ocular surgery or ocular radiation therapy; (3) Wearing contact lens; (4) Pre-existing ocular surface or inflammatory eye diseases, lacrimal duct disorders, eyelid conditions, or ocular trauma; (5) Use of medications other than anti-thyroid drugs that could potentially induce or exacerbate dry eye; (6) Other autoimmune diseases that could lead to dry eye and severe systemic illnesses.

Recorded data included gender, age, BMI, smoking history, hypertension history, diabetes history, thyroid disease history, anti-thyroid medication usage, history of 131I therapy, history of thyroid surgery, ocular disease history and medication usage, GO disease course and treatment history, as well as other systemic medical history and medication usage. Symptoms such as spontaneous retrobulbar pain, pain during eye movement, and diplopia (intermittent or continuous) were also documented.

2.4. IVCM examination data collection

The microstructures of MGs in all study subjects were examined using the HRT3 IVCM from Heidelberg Engineering, Germany. After surface anesthesia (0.4% oxybuprocaine), the lower eyelid MGs structures were observed. Images were captured in the nasal, central,

and temporal regions of the lower eyelid and saved. The evaluation criteria included the following parameters: meibomian gland orifice area (MOA), meibomian gland acinar density (MAD), meibomian gland acinar longest diameter (MALD), meibomian gland acinar shortest diameter (MASD), meibomian gland acinar irregularity (MAI), meibum secretion reflectivity (MSR), acinar wall inhomogeneity (AWI), acinar periglandular interstices inhomogeneity (API), and severity of meibomian gland fibrosis (MF). The schematic diagram of each indicator has provided in Fig. 1. The detailed scoring criteria for MAI, MSR, AWI, API, and MF are provided in Supplement 1 [19–22]. For each eye, three non-overlapping MGs images were randomly selected from each of the three regions. Analysis was performed using ImageJ software (version 1.8.0). The final calculation involved obtaining the average values of each parameter. Two different observers independently conducted the calculations and statistics for each structure, with the results being averaged.

Statistical analysis

All eligible patients were randomly divided into training and validation datasets in a 6:4 ratio. Continuous variables, presented as means \pm standard deviations (SD) or medians (ranges), were compared using the two-sample t-test or Wilcoxon's rank-sum test. Categorical variables were reported as percentages and compared using the Pearson's chi-squared test or Fisher's exact test.

Based on the training cohort, the least absolute shrinkage and selection operator (LASSO) method was used to select the best subset of risk factors based on the IVCM examination data, a diagnostic model for evaluating the activity of GO was developed.

The discrimination of the model was using the area under the receiver operating characteristic curve (AUC) involving the Delong test, net reclassification improvement (NRI), and integrated discrimination improvement (IDI) methods. Calibration was evaluated using the Hosmer-Lemeshow chi-square statistic and calibration plot. Then, a nomogram for the model was established. All statistical tests were two-sided, and $P < 0.05$ was considered statistically significant. Data analyses were performed using R (version 4.0.4, R Foundation for Statistical Computing, Vienna, Austria).

Result

Patient characteristics

A total of 45 GO patients, corresponding to 90 eyes, were included in this study. Among them, 49 eyes exhibited characteristics of the inactive phase, while 41 eyes showed features of the active phase. The median age of GO patients was 51 years (range: 28–61). There were 23 female patients (51.11%) and 22 male patients (48.89%).

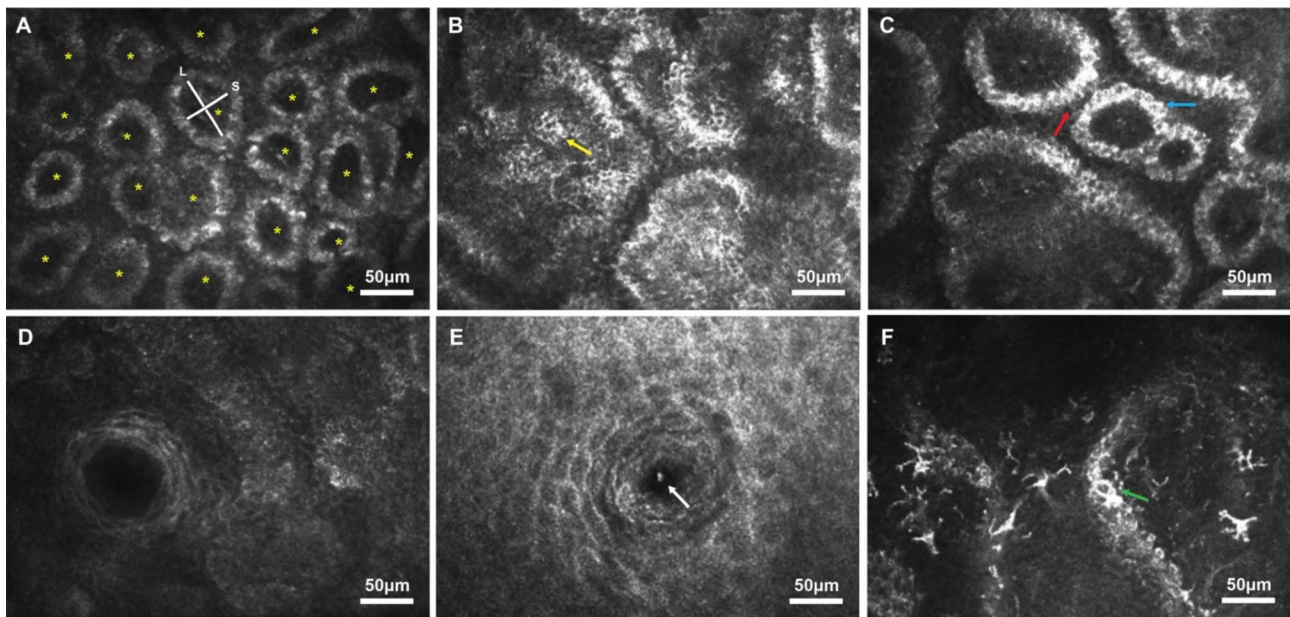


Fig. 1 Representative images illustrating MGs structure and function of IVCM **(A)** Morphology and distribution pattern of MGs acinus in patients without GO, * representing cell counts used for measuring MAD, L representing MALD, and S representing MASD; **(B)** Decreased MGs acinar density in GO patients, exhibiting irregular and markedly expanded and fused acini; yellow arrows indicate highly reflective secretion within the acini; **(C)** Red arrows indicate high reflectivity in the acinar interstices, and blue arrows indicate high reflectivity in the acinar walls; **(D)** Regular and elliptical opening of the MGs orifices in patients without GO; **(E)** Irregular morphology and reduced area of MGs orifices in GO patients; white arrows indicate the presence of highly reflective secretion blocking the MGs orifices; **(F)** Green arrows indicate focal fibrous structures in MGs

The mean BMI was 23.5 kg/m² (range: 23.0–24.1). Smoking history was reported in 16 patients (17.78%), while 74 (82.22%) were non-smokers. Hypertension was present in 21 patients (23.33%), with comparable prevalence in both phases. Diabetes was rare, affecting only 2 patients (2.22%), both in the inactive phase. Thyroid function abnormalities were prevalent (91.11%), with 95.1% in the active phase versus 87.8% in the inactive phase. A significant disparity was observed in I¹³¹ therapy history, with 53.7% of active-phase patients compared to 12.2% in the inactive phase. Thyroid surgery history was exclusively reported in the inactive phase. Anti-thyroid medication usage was more frequent in the active phase (95.1% vs. 69.4%) (Table 1).

Construction of models

Table 2 provide an overview of the baseline values of microstructural and functional indicators of MGs, which were acquired through IVCM examinations on a cohort of 90 eyes from GO patients. These data were used in the process of selecting predictor variables. The study focused on the CAS associated with GO and employed nine IVCM-detected indicators: MOA, MAD, MALD, MASD, MAI, MSR, AWI, API, and severity of MF as predictive features. For the purpose of predictor variable selection, a Lasso regression algorithm was utilized, which ultimately resulted in the inclusion of five predictor variables: MAD, MSR, API, AWI, and Severity of MF

(Fig. 2). Subsequently, a logistic regression model was constructed, and the results are presented in Fig. 3. As depicted in the Fig. 4, the AUC for the training set model reached 0.959 [95% confidence interval (CI): 0.914–1], and the AUC for the validation set was 0.969 (95% CI: 0.916–1). In terms of calibration, both the training set and validation set models demonstrated high accuracy (P_{train} = 0.9925; P_{test} = 0.6258) (Fig. 5).

Construction of nomogram

A nomogram chart was constructed to visualize the logistic regression model based on microstructural indicators of Meibomian glands (Fig. 6). This column chart comprises a total of 8 axes, where axes 2 to 6 represent the five variables in the regression equation: MAD, MSR, AWI, API, and MF. Each axis is labeled with corresponding scales, representing the range of possible values for each variable, while the length of the line segments reflects the contribution of each variable to predicting the active phase of GO. Therefore, based on the labels and scales of the five variable axes, one can calculate the predictive scores for each variable (i.e., the scores corresponding to axis 1). The predictive scores for the five variables are then summed to obtain the total score on axis 7, and the probability of predicting GO in the active phase is determined based on the total score on the lowermost axis 8. The column chart enhances the interpretability of the diagnostic model's results, facilitating rapid

Table 1 Baseline clinical characteristics of the 45 patients, corresponding to 90 eyes with GO, stratified using the CAS

Characteristic	Total (90 eyes)	CAS ≥ 3 (41 eyes)	CAS < 3 (49 eyes)	P-value
Age - years				
Median (range)	51 (28–61)	53 (28–61)	46 (28–61)	< 0.001
Gender - n (%)				
Men	44 (48.9)	23 (56.1)	21 (42.9)	0.108
Women	46 (51.1)	18 (43.9)	28 (57.1)	
BMI - kg/m²				
Means (± standard deviations)	23.5 (23.0–24.1)	23.6 (22.7–24.5)	23.5 (22.7–24.2)	0.791
Smoking history- n (%)				
No	74 (17.78)	36 (87.8)	38 (77.6)	0.205
Yes	16 (82.22)	5 (12.2)	11 (22.4)	
Hypertension history - n (%)				
No	69 (76.67)	31 (75.6)	38 (77.6)	0.828
Yes	21 (23.33)	10 (24.4)	11 (22.4)	
Diabetes history - n (%)				
No	88 (97.78)	41 (100.0)	47 (95.9)	0.498 [#]
Yes	2 (2.22)	0 (0.0)	2 (4.1)	
Thyroid function - n (%)				
Normal	8 (8.89)	2 (4.9)	6 (12.2)	0.283 [#]
Abnormal	82 (91.11)	39 (95.1)	43 (87.8)	
I¹³¹therapy history - n (%)				
No	62 (68.89)	19 (46.3)	43 (87.8)	< 0.001
Yes	28 (31.11)	22 (53.7)	6 (12.2)	
Thyroid surgery history - n (%)				
No	84 (93.33)	41 (100.0)	43 (87.8)	0.030 [#]
Yes	6 (6.67)	0 (0.0)	6 (12.2)	
Anti-thyroid medication usage - n (%)				
No	17 (18.89)	2 (4.9)	15 (30.6)	0.002 [#]
Yes	73 (81.11)	39 (95.1)	34 (69.4)	

CAS=Clinical Activity Score; Range=min–max. P-values are for comparisons between the active phase of graves' orbitopathy(GO) (CAS ≥ 3)and the inactive phase of GO(CAS < 3). [#]Fisher's exact test: Used for categorical variables with expected counts < 5

assessment and diagnosis of the activity of GO in clinical practice.

Discussion

An effective and reliable method for assessing the activity of GO is essential not only for guiding GO treatment but also for evaluating treatment outcomes and prognosis for GO patients [9]. Therefore, the exploration of an effective diagnostic model for staging GO disease activity is of paramount clinical significance. While the CAS is gradually gaining acceptance among ophthalmologists worldwide, it can yield varying results depending on the assessor, which may hinder its precision. Additionally, GO patients are typically initially assessed by endocrinologists or primary care physicians, which may further compromise the accuracy and consistency of CAS scoring.

In our previous research [16], we observed a correlation between microstructural indicators of MGs, as detected through IVCN, and CAS. These indicators exhibited differences between the active and quiescent phases of GO. Thus, in this study, we leveraged IVCN

to collect quantifiable data on changes in the microstructure of MGs in GO patients. With this dataset of 45 patients, totaling 90 eyes, we constructed a diagnostic model for GO activity. This model utilized the IVCN-detected microstructural indicators of MGs, including MOA, MAD, MALD, MASD, MAI, MSR, AWI, API, and ME, to evaluate their relationship with the activity of GO in patients.

To our knowledge, we are the first to use IVCN-detected MGs indicators as predictive factors for assessing GO activity. Prior research by Jae Hoon Moon et al. [23] developed a machine learning (ML)-assisted system that used digital facial images to mimic an expert's CAS assessment, achieving sensitivities of 72.7% and specificities of 83.2% for diagnosing active GO. Chenyi Lin et al. [24] established a deep convolutional neural network to automatically detect GO activity from MRI images. Jun Soo Byun et al. [25] created a logistic regression predictive model based on multiple MRI features of lacrimal glands (LG) with an AUC of 0.94. Wang, Minghui et al. [26] used clinical characteristics and hematological

Table 2 The characteristics of meibomian gland structure and function of included patients

Variable	Total (N= 90 eyes)	Inactive group (N= 49 eyes)	Active group (N= 41 eyes)	P-value
MOA	1672.00 (1153.00 ~ 2444.75)	1699.00 (1310.00 ~ 2694.00)	1643.00 (1104.00 ~ 2170.00)	0.630*
MAD	85.51 ± 35.35	93.59 ± 39.09	75.85 ± 27.78	0.028†
MALD	116.91 ± 28.99	119.31 ± 27.72	114.05 ± 30.53	0.267†
MASD	41.59(31.85 ~ 54.69)	42.45(34.54 ~ 54.71)	39.12(29.78 ~ 54.56)	0.598*
MAI				0.012#
0	1(1.11%)	1(2.04%)	0(0.00%)	
1	53(58.89%)	34(69.39%)	19(46.34%)	
2	32(35.56%)	14(28.57%)	18(43.90%)	
3	4(4.44%)	0(0.00%)	4(9.76%)	
MSR				< 0.001#
0	1(1.11%)	1(2.04%)	0(0.00%)	
1	49(54.44%)	17(34.69%)	32(78.05%)	
2	32(35.56%)	23(46.94%)	9(21.95%)	
3	8(8.89%)	8(16.33%)	0(0.00%)	
AWI				< 0.001#
0	12(13.33%)	12(24.49%)	0(0.00%)	
1	44(48.89%)	31(63.27%)	13(31.71%)	
2	22(24.44%)	6(12.24%)	16(39.02%)	
3	12(13.33%)	0(0.00%)	12(29.27%)	
API				< 0.001#
0	10(11.11%)	10(20.41%)	0(0.00%)	
1	37(41.11%)	28(57.14%)	9(21.95%)	
2	31(34.44%)	11(22.45%)	20(48.78%)	
3	12(13.33%)	0(0.00%)	12(29.27%)	
MF				0.005#
0	25(27.78%)	7(14.29%)	18(43.90%)	
1	56(62.22%)	37(75.51%)	19(46.34%)	
2	9(10.00%)	5(10.20%)	4(9.76%)	

MOA=Meibomian gland orifice area; MAD=Meibomian gland acinar density; MALD=Meibomian gland acinar longest diameter; MASD=Meibomian gland acinar shortest diameter; MAI=Meibomian gland acinar irregularity; MSR=Meibum secretion reflectivity; AWI=Acinar wall inhomogeneity; API=Acinar periglandular interstices inhomogeneity; MF=Severity of Meibomian gland fibrosis; P-values are for comparisons between the inactive phase of graves' orbitopathy(GO) and the active phase of GO. Data is presented as medians (Q1 ~ Q3), means (± standard deviation), or n (%). Statistical analyses were performed using the following tests: * Mann-Whitney U test; † independent samples t-test; # chi-square test

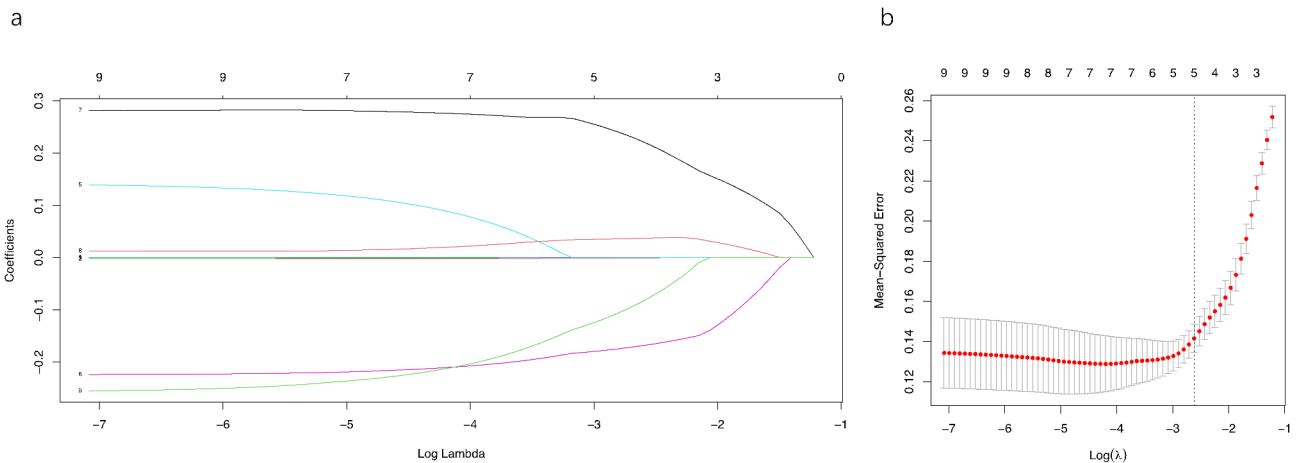


Fig. 2 (a) LASSO coefficient profiles of the 9 indicators of MGs obtained through IVCN. (b) Five indicators selected using LASSO Cox regression analysis. The dotted vertical line was drawn at the optimal scores by 1-s.e. criteria

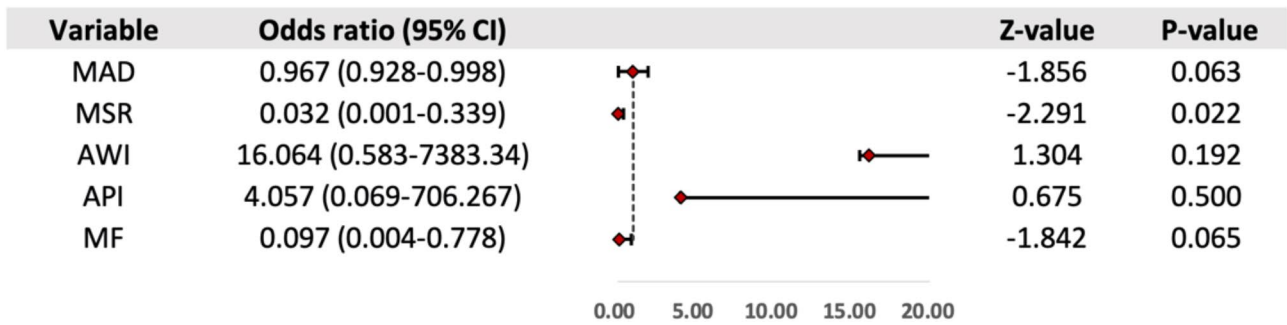


Fig. 3 Multivariate logistic regression analysis for the combined model. CI: confidence interval; MAD=Meibomian gland acinar density; MSR=Meibum secretion reflectivity; AWI=Acinar wall inhomogeneity; API=Acinar periglandular interstices inhomogeneity; MF=Severity of Meibomian gland fibrosis

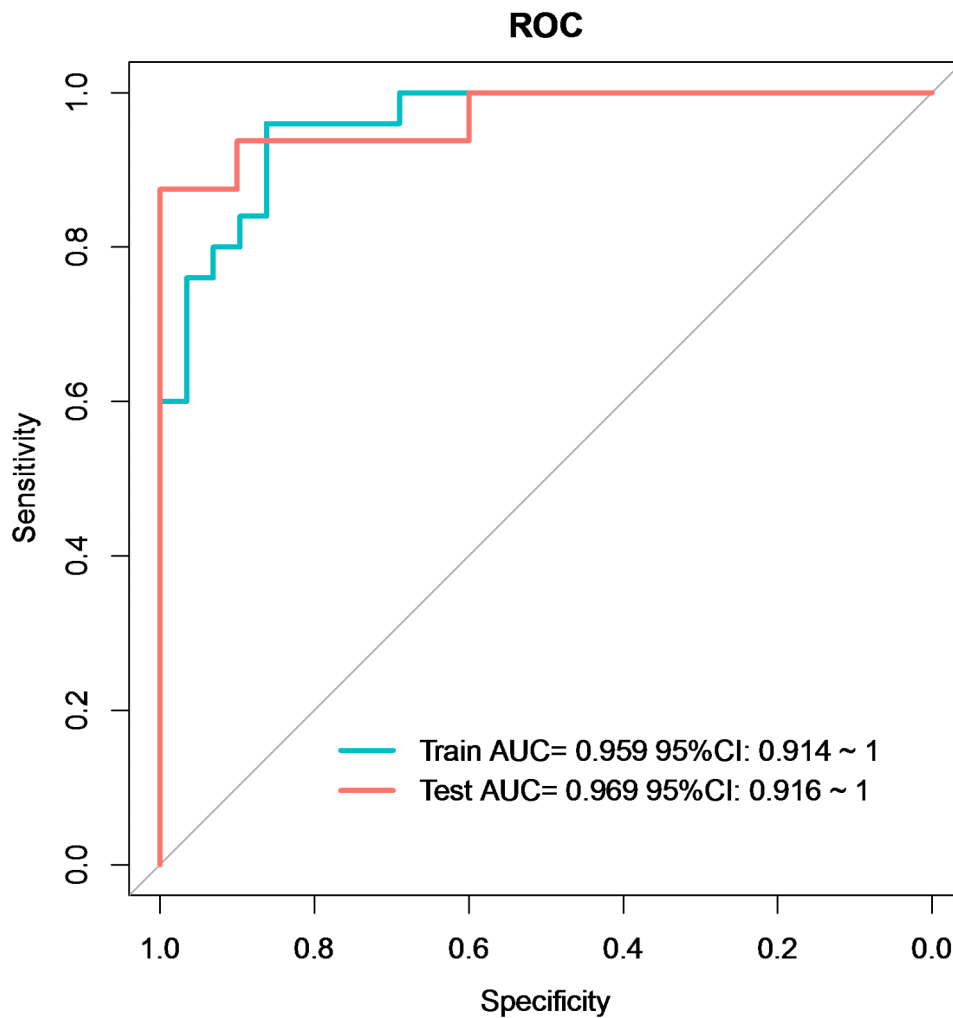


Fig. 4 The areas under the receiver operating characteristic curve (AUC) of models in the training dataset and the validation dataset

indices as predictive variables to build a random forest model for assessing GO activity. Our study diverges by focusing on quantifiable ocular surface feature changes and employing the non-invasive (feasible and cost-effective) IVCMD detection method, which contributes to the development of a new model for predicting GO activity.

Our research provides a new approach for evaluating the activity of GO. The predictive model we established achieved an AUC of 0.959 (95% CI: 0.914-1) for the training set and an AUC of 0.969 (95% CI: 0.916-1) for the validation set. The close AUC values between the training and validation sets indicate strong repeatability and generalizability of the model, making it a valuable tool for

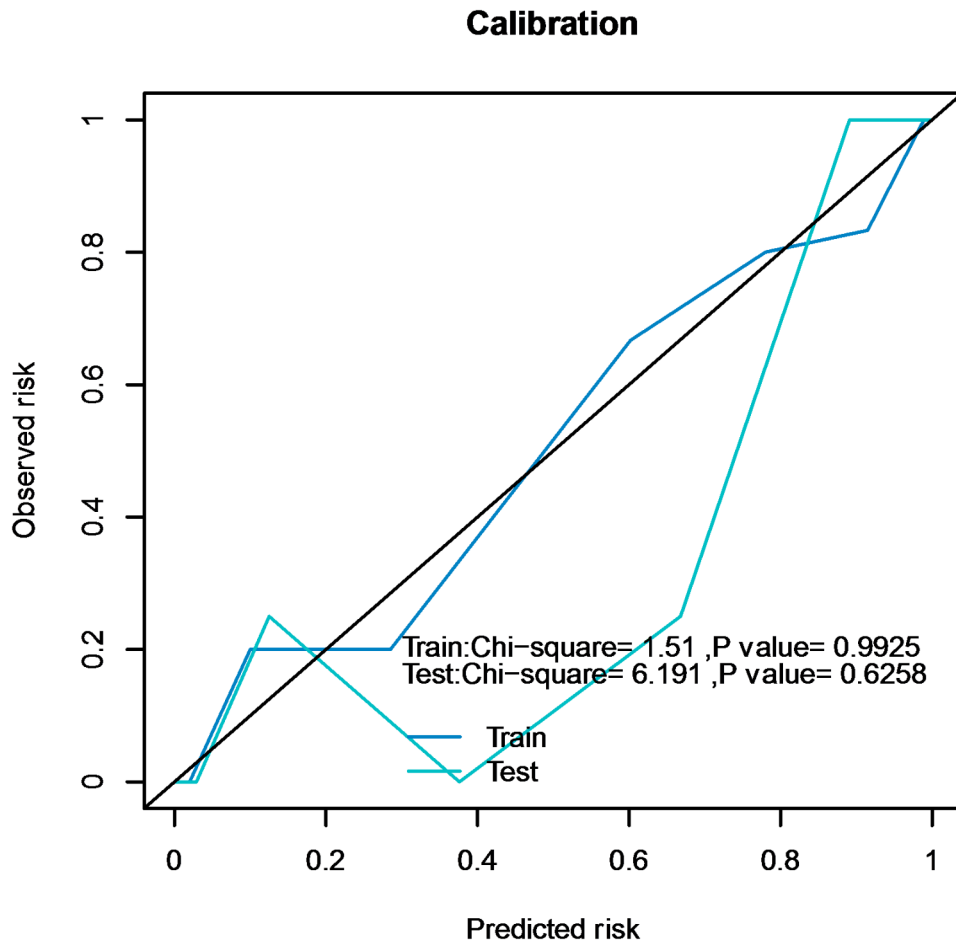


Fig. 5 Calibration curve of the models in the training dataset and the validation dataset

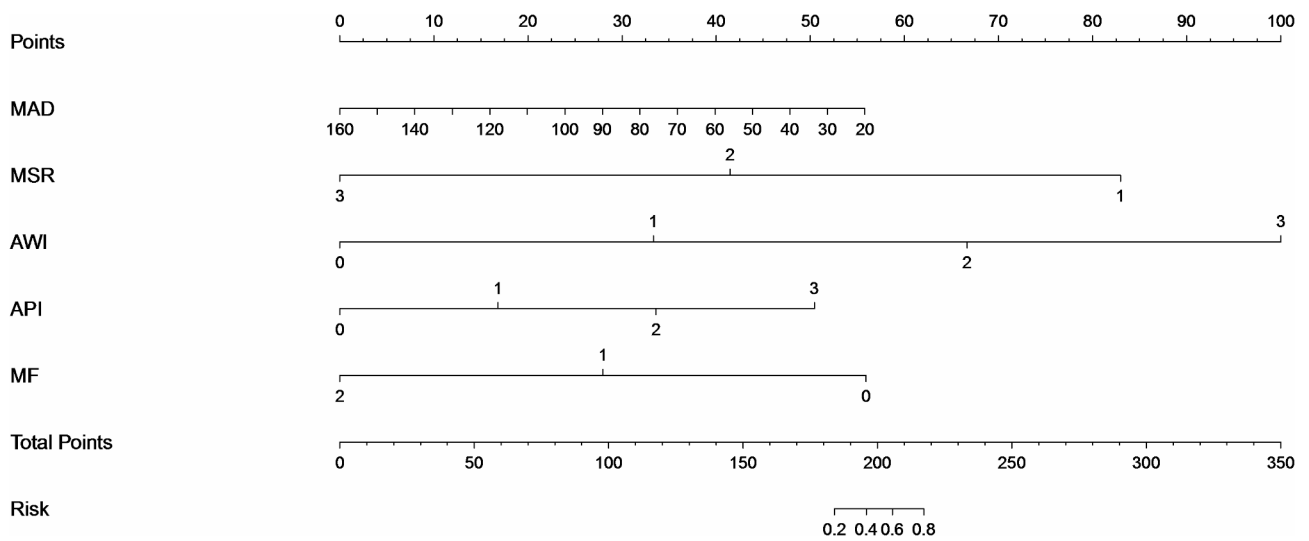


Fig. 6 Nomogram for predicting GO activity

assisting in GO diagnosis. Additionally, this model aids CAS in evaluating active and quiescent phases of GO that may not be distinguishable based solely on typical symptoms and signs. Moreover, due to the objectivity and consistency of IVCN results, we hope to employ this model in assessing treatment responses in future research.

Nonetheless, our study has certain limitations. Firstly, to alleviate discomfort and optimize participant cooperation for clear MGs microstructural imaging, IVCN examinations were conducted exclusively on the lower eyelids, although changes in both upper and lower eyelids may influence ocular surface conditions. Secondly, our research is cross-sectional, and the grouping criteria used are relatively subjective, relying on CAS scores. Long-term follow-up and validation of patients' progress are needed. Therefore, in the future, we aim to collect multimodal data, including imaging and hematological parameters, to further refine the model. Lastly, our study only included Chinese patients, which may limit the generalizability of the results to other ethnic groups. Therefore, we plan to expand the sample size and conduct multicenter external validation to enhance the model's accuracy.

In summary, the model constructed based on microstructural indicators of MGs obtained through IVCN, including MAD, MSR, AWI, API, and MF, offers significant clinical utility for assessing GO disease activity. Its visual nomogram facilitates rapid assessment and judgment of GO disease activity in clinical practice.

Supplementary Information

The online version contains supplementary material available at <https://doi.org/10.1186/s12902-025-01895-3>.

Supplementary Material 1

Acknowledgements

NA.

Author contributions

FGJ and XHW were responsible for the concept and design of the study, interpretation of data, and revising of the article. ZXS, YYY and SNC were contributed equally to the manuscript as joint first authors. The other authors were responsible for interpretation of data and revision of the intellectual content. All authors participated in final approval of the article and agreed to be accountable for all aspects of the work.

Funding

This work was supported by "the Fundamental Research Funds for the Central Universities" (YCJK20230109) and "the Key Research and Development Program of Hubei Province" (2023BCB147). The funding organization had no role in the design or conduct of this study.

Data availability

No datasets were generated or analysed during the current study.

Declarations

Ethics approval and consent to participate

The authors are accountable for all aspects of the work in ensuring that questions related to the accuracy or integrity of any part of the work are

appropriately investigated and resolved. All procedures performed in this study were in accordance with the Declaration of Helsinki. The study was conducted following the approval obtained from the Institutional Review Board of Union Hospital, Tongji Medical College, Huazhong University of Science and Technology, approval number 20220293. Clinical trial number: not applicable.

Competing interests

The authors declare no competing interests.

Conflict of interest

All authors declare no conflicts of interest.

Author details

¹Department of Ophthalmology, Union Hospital, Tongji Medical College, Huazhong University of Science and Technology, Wuhan 430030, Hubei, China

²Department of Ophthalmology, Affiliated Jinhua Hospital, Zhejiang University School of Medicine, Jinhua 321000, Zhejiang, China

³Department of Ophthalmology, Tongji Medical College, Wuhan Hospital of Traditional Chinese and Western Medicine, Huazhong University of Science and Technology, Wuhan No.1 Hospital, Wuhan, China

⁴Department of Biostatistics, School of Public Health, Southern Medical University, Guangzhou 510515, China

Received: 24 February 2024 / Accepted: 6 March 2025

Published online: 26 March 2025

References

1. Li B, et al. A new radiological measurement method used to evaluate the modified transconjunctival orbital fat decompression surgery. *BMC Ophthalmol.* 2021;21(1):176.
2. Chen H, et al. Thyroid-Associated orbitopathy: evaluating microstructural changes of extraocular muscles and optic nerves using Readout-Segmented Echo-Planar imaging-Based diffusion tensor imaging. *Korean J Radiol.* 2020;21(3):332–40.
3. Hodgson N, Rajaii F. Current Understanding of the progression and management of thyroid associated orbitopathy: A systematic review. *Ophthalmol Therapy.* 2020;9(1):21–33.
4. Wu L, et al. Observation of corneal Langerhans cells by in vivo confocal microscopy in Thyroid-Associated ophthalmopathy. *Curr Eye Res.* 2016;41(7):927–32.
5. Villani E, et al. Corneal involvement in graves' orbitopathy: an in vivo confocal study. *Investig Ophthalmol Vis Sci.* 2010;51(9):4574–8.
6. Lai EW et al. The association between autoimmune thyroid disease and ocular surface damage: A retrospective Population-Based cohort study. *J Clin Med.* 2023. 12(9).
7. Rana HS, et al. Ocular surface disease in thyroid eye disease: A narrative review. *Ocul Surf.* 2022;24:67–73.
8. Kashkoul MB, et al. Subjective versus objective dry eye disease in patients with moderate-severe thyroid eye disease. *Ocul Surf.* 2018;16(4):458–62.
9. Bartalena L, et al. The 2021 European group on graves' orbitopathy (EUGOGO) clinical practice guidelines for the medical management of graves' orbitopathy. *Eur J Endocrinol.* 2021;185(4):G43–67.
10. Mourits MP et al. Clinical activity score as a guide in the management of patients with Graves' ophthalmopathy. *Clin Endocrinol.* 1997. 47(1).
11. Giannaccare G, et al. In vivo confocal microscopy morphometric analysis of corneal Subbasal nerve plexus in dry eye disease using newly developed fully automated system. Volume 257. *Graefe's Archive for Clinical and Experimental Ophthalmology*; 2019. pp. 583–9. 3.
12. Liu Y et al. *Observation of Conjunctiva-Associated Lymphoid Tissue With In Vivo Confocal Microscopy in Healthy Patients and Patients With Meibomian Gland Dysfunction.* *Cornea.* 2022. 41(9): pp. 1129–1136.
13. Wu L, et al. Altered corneal nerves in Chinese Thyroid-Associated ophthalmopathy patients observed by in vivo confocal microscopy. *Med Sci Monit.* 2019;25:1024–31.
14. Wei YH, et al. In vivo confocal microscopy of bulbar conjunctiva in patients with graves' ophthalmopathy. *J Formos Med Assoc.* 2015;114(10):965–72.

15. Wu LQ et al. *Observation of Corneal Langerhans Cells by In Vivo Confocal Microscopy in Thyroid-Associated Ophthalmopathy*. *Current Eye Research*, 2016. 41(7): pp. 927–32.
16. Cheng S, et al. *In vivo confocal microscopy assessment of meibomian glands microstructure in patients with graves' orbitopathy*. *BMC Ophthalmol*. 2021;21(1):261.
17. Vagge A, et al. *In vivo confocal microscopy morphometric analysis of meibomian glands in patients with graves ophthalmopathy*. *Cornea*. 2021;40(4):425–9.
18. Bartley GB, Gorman CA. *Diagnostic criteria for graves' ophthalmopathy*. *Am J Ophthalmol*. 1995;119(6):792–5.
19. Villani E, et al. *In vivo confocal microscopy of meibomian glands in Sjögren's syndrome*. *Investig Ophthalmol Vis Sci*. 2011;52(2):933–9.
20. Villani E, et al. *In vivo confocal microscopy of meibomian glands in contact lens wearers*. *Investig Ophthalmol Vis Sci*. 2011;52(8):5215–9.
21. Ban Y, et al. *Morphologic evaluation of meibomian glands in chronic graft-versus-host disease using in vivo laser confocal microscopy*. *Mol Vis*. 2011;17:2533–43.
22. Lin T, Gong L. *Vivo confocal microscopy of meibomian glands in primary blepharospasm: A prospective case-control study in a Chinese population*. *Medicine*. 2016;95(23):e3833.
23. Moon JH, et al. *Machine learning-assisted system using digital facial images to predict the clinical activity score in thyroid-associated orbitopathy*. *Sci Rep*. 2022;12(1):22085.
24. Lin C, et al. *Detection of active and inactive phases of thyroid-associated ophthalmopathy using deep convolutional neural network*. *BMC Ophthalmol*. 2021;21(1):39.
25. Byun JS, Moon NJ, Lee JK. *Quantitative analysis of orbital soft tissues on computed tomography to assess the activity of thyroid-associated orbitopathy*. *Graefes Archive Clin Experimental Ophthalmol = Albrecht Von Graefes Archiv Fur Klinische Und Experimentelle Ophthalmologie*. 2017;255(2):413–20.
26. Wang M, et al. *Using the random forest algorithm to detect the activity of graves orbitopathy*. *J Craniofac Surg*. 2023;34(2):e167–71.

Publisher's note

Springer Nature remains neutral with regard to jurisdictional claims in published maps and institutional affiliations.